# RESEARCH ON THE SPATIOTEMPORAL DISTRIBUTION OF $XCO_2$ EMISSIONS BASED ON GOSAT SATELLITES IN CHINA

Xinyan Hou[1] , Hasi Bagan[1] ,Terigelehu Te[1] Bayarsaikhan Uudus[2] and Qinxue Wang[3]
[1]Shanghai Normal University, No.100, Guilin Road, Xuhui District, Shanghai 200234, China,
Email: 1000512115@smail.shnu.edu.cn
[1]Shanghai Normal University, No.100, Guilin Road, Xuhui District, Shanghai 200234, China,
Email: hasibagan@staff.shnu.edu.cn
[1]Shanghai Normal University, No.100, Guilin Road, Xuhui District, Shanghai 200234, China,
Email: 1000529963@smail.shnu.edu.cn
[2]National University of Mongolia, Ulaanbaatar 210646, Mongolia,
Email: bayaraa@num.edu.mn
[3]National Institute for Environmental Studies, Tsukuba, Ibaraki 305-8506, Japan,
Email: wangqx@nies.go.ip

**KEY WORDS:** GOSAT-2; $XCO_2$; Spatial distribution; China

**ABSTRACT:** Carbon dioxide ($CO_2$) is the largest greenhouse gas (GHG). Carbon dioxide emissions have attracted worldwide attention. At present, carbon satellite observation is an important means to study and analyze the global carbon cycle. This study mainly uses ordinary Kriging interpolation technology to analyze the temporal and spatial changes of carbon dioxide column concentration in 2020 and 2021 based on Level 2 GOSAT-2 satellite data (GOSAT-2 TANSO-FTS-2 SWIR L2 Column-averaged Dry-air Mole Fraction Product). The conclusion is that the spatial distribution of China column average $CO_2$ ($XCO_2$) is higher in Southeast China and lower in Northwest China. The lowest and highest values in 2020 appeared in summer, the lowest value is 389.6 ppm and the highest value is 448.8 ppm. The lowest and highest values in 2021 appeared in winter and spring, the lowest value is 388.5 ppm and the highest value is 452.1 ppm. The overall level of $XCO_2$ in 2021 is higher than that in 2020. $XCO_2$ is increasing year by year in China. The average value of $XCO_2$ increased from 414.2 ppm in 2020 to 417.9 ppm in 2021, an increase of 3.7 ppm. In areas with dense construction land, $XCO_2$ increased steadily. Subsequent studies will focus on the correlation between $XCO_2$ and other factors affecting the increase of concentration, such as wind speed, wind direction, land surface temperature (LST), Normalized Difference Vegetation Index (NDVI), air temperature, humidity and other environmental variables. It will also be further explored in combination with the carbon dioxide concentration observed on the ground.

## 1. INTRODUCTION

The Japanese Greenhouse gases Observing SATellite (GOSAT) in orbit since 23 January 2009 (Kuze et al., 2009). GOSAT-2 (Greenhouse gases Observing Satellite-2), which is also known as "IBUKI-2", is a JAXA satellite dedicated to the observation of greenhouse gases. The satellite expands upon the capabilities of its predecessor, and carries enhanced versions of the two mission instruments aboard the GOSAT satellite, TANSO-FTS-2 (Thermal And Near infrared Sensor for carbon Observation-Fourier Transform Spectrometer-2) and TANSO-CAI-2 (Cloud and Aerosol Imager-2) (Suto et al., 2021). By analyzing the GOSAT and GOSAT-2 satellite observations of greenhouse gases, scholars and scientists will be able to determine and analyze the global and spatial-temporal distribution of carbon dioxide ($CO_2$) and methane ($CH_4$), as well as detect how the sources and sinks of these gases vary with season, year and place. For example, relevant scholars use the high-resolution inversion model of GOSAT and ground observation to analyze methane emission on a national scale (Janardanan et al., 2020). The new findings will enhance scientific understanding of the causes of global warming. In addition, the GHG data obtained from the analysis will provide some help and data support for improving climate change prediction and developing reasonable plans to mitigate global warming. Satellite-based $XCO_2$ (column-averaged $CO_2$) carries large amounts of information from the bottom atmospheric layer (near-ground) to the top of the atmosphere, including background atmospheric $CO_2$ (Deng et al., 2014, Hwang et al., 2016). Many countries have successively launched satellites to monitor greenhouse gas emissions. The TanSat, GOSAT, and OCO-2 and OCO-3 instruments are still operating, and several different retrieval algorithms have been developed to derive $XCO_2$ from their near-infrared (NIR) and shortwave infrared (SWIR) spectra (Noël et al., 2021). The purpose of this paper is to study the spatial and temporal distribution characteristics of atmospheric $CO_2$ column concentration monitored by GOSAT-2 in China.

## 2. MATERIALS AND METHODS

### 2.1 Study Area

China, officially the People's Republic of China (PRC), is a country in East Asia. It is the world's most populous country with a population exceeding 1.4 billion people. Covering an area of approximately 9.6 million square kilometers (3,700,000 sq mi), it is the world's third or fourth largest country. The country consists of 23 provinces, five autonomous regions, four municipalities, and two Special Administrative Regions (Hong Kong and Macau). The national capital is Beijing, and the most populous city and financial center is Shanghai.

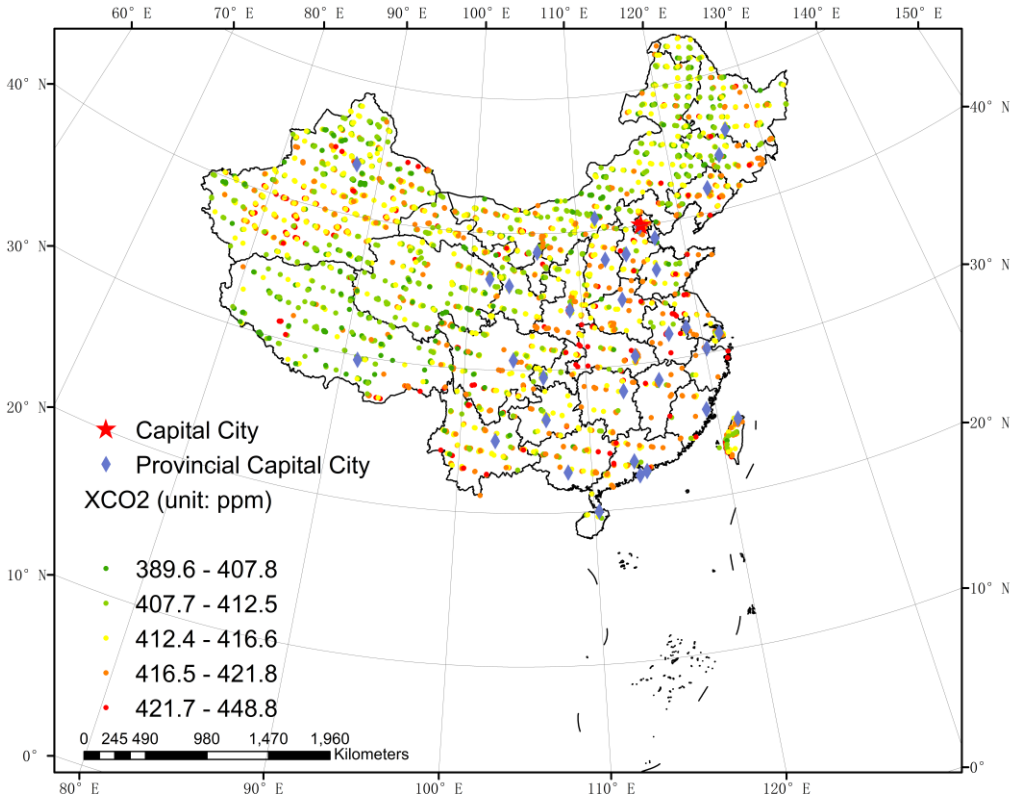


Figure.1 Location of the study area and position of GOSAT-2 column

**2.2 Satellite Data**

GOSAT-2 satellite monitored some areas of China, with the main observation points concentrated in the urban area of China. GOSAT-2 Level -2 product (GOSAT-2 TANSO-FTS-2 SWIR L2 Column-averaged Dry-air Mole Product) was used in this study, and the study period was from June 2020 to May 2021.

## 3. RESULTS

### 3.1 Statistical analysis of GOSAT-2 $XCO_2$

GOSAT-2 provides the column abundance of $CO_2$ (the number of the gas molecule in a vertical unit column). The sample sizes in 2020 and 2021 are relatively sufficient. The mean $XCO_2$ in China showed a trend of continuous increase from 410.72 ppm to 421.00 ppm From June 2020 to May 2021. $XCO_2$ in the study area remained above 389.61 ppm, and $XCO_2$ was at a high level. The $XCO_2$ is increasing year by year in China, especially in the summer of 2021. From 2020 to 2021, the $XCO_2$ reached the peak in January 2021. The overall level of $XCO_2$ in 2021 is higher than that in 2020. The average value of $XCO_2$ increased from 413.86 ppm in 2020 to 419.59 ppm in 2021, an increase of 5.73 ppm (Table 1).

Table 1. Descriptive statistics of GOSAT-2 $XCO_2$ from 2020 to 2021 in China

| Year | Month | Min(ppm) | Max(ppm) | Mean(ppm) | Number of samples |
|---|---|---|---|---|---|
| 2020 | 6 | 392.45 | 448.80 | 414.74 | 640 |
| | 7 | 389.61 | 428.59 | 410.72 | 768 |
| | 8 | 392.05 | 431.76 | 412.83 | 989 |
| | 9 | 389.98 | 442.98 | 413.08 | 914 |
| | 10 | 394.83 | 439.19 | 414.29 | 1227 |
| | 11 | 400.43 | 430.22 | 414.21 | 1013 |
| | 12 | 394.39 | 430.95 | 417.17 | 695 |
| 2021 | 1 | 398.84 | 435.42 | 418.51 | 839 |
| | 2 | 404.44 | 438.39 | 417.36 | 836 |
| | 3 | 396.85 | 444.19 | 420.12 | 499 |
| | 4 | 405.17 | 442.03 | 421.00 | 659 |
| | 5 | 402.20 | 439.65 | 420.97 | 665 |

### 3.2 Visualization Analysis of GOSAT-2 $XCO_2$

In order to visualize $XCO_2$ in China, we performed interpolation analysis on GOSAT-2 data. Visualized GOSAT-2 data were generated for monthly data from June 2020 to May 2021 using ordinary Kriging interpolation method, and spatial distribution of $XCO_2$ was visualized on regional and time scales (Figure 2).

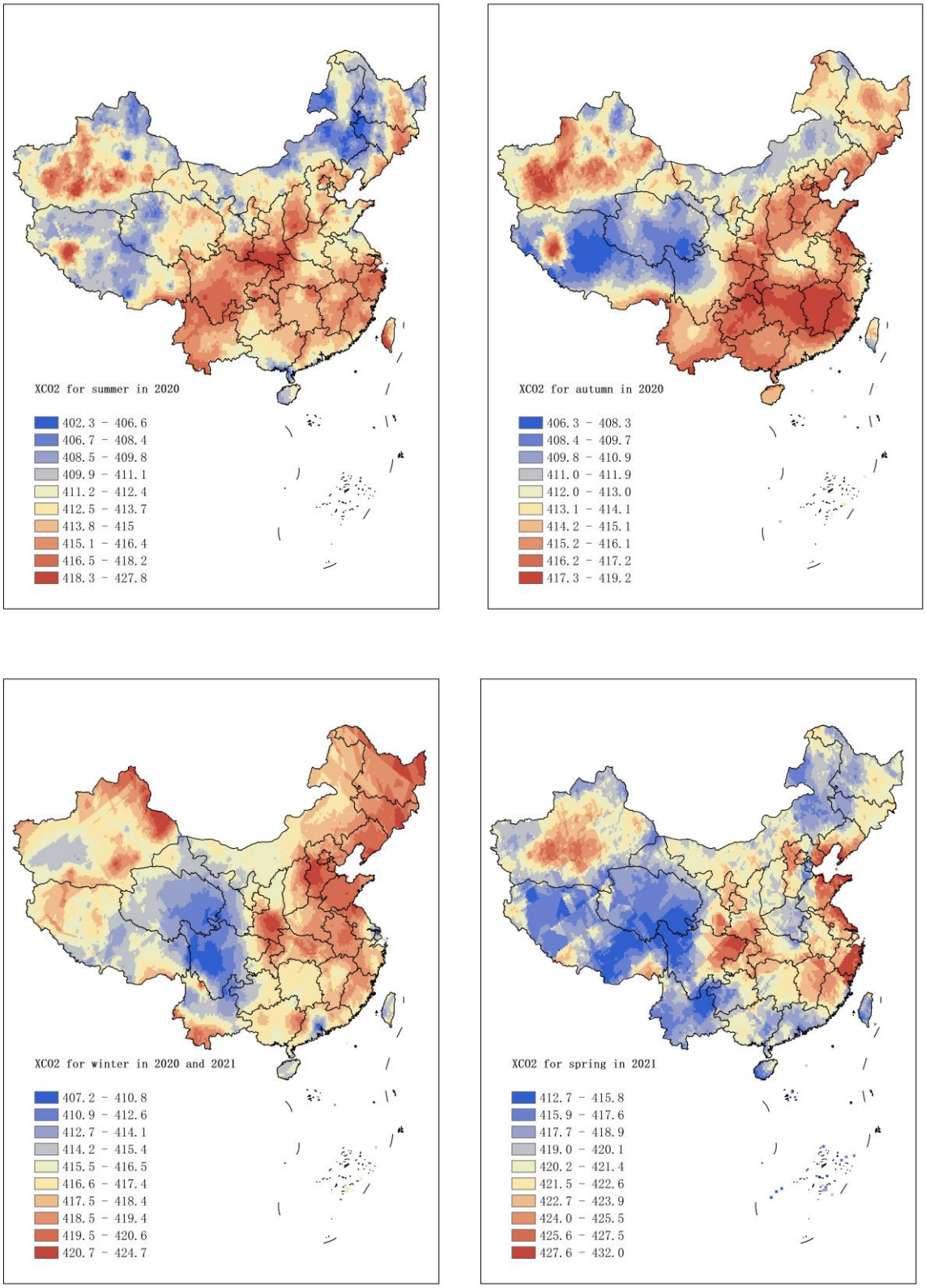


Figure.2 Spatial distribution of $XCO_2$ in spring, summer, autumn and winter of 2020 and 2021 (Ordinary Kriging interpolation method)

Cross-validation is commonly used to validate how good the kriging model interpolates by comparing the estimated values with the observed values (Gong et al., 2014). The accuracy of Ordinary kriging interpolation is verified from four parameters: Root Mean Square (RMSE), Average Standard Error (ASE), Root Mean Square Standardized Error (RMSSE), Mean Standardized Error (MSE). RMSE provides a measure of interpolation accuracy, with a lower RMSE representing a more accurate estimate. In this study, ASE was distributed in the range of 3.333 - 4.889 (ppm), while RMSE was in the range of 3.257 - 4.503 (ppm). The ASE value was close to the root mean square error, meaning that the variability in the prediction was correctly assessed. The results of this study showed that ASE was close to RMSE, and the error level was acceptable due to the normal sample size. The root mean square error is calculated by dividing the root mean square error by ASE. An RMSSE close to 1 indicates fewer prediction standard errors, an MSE close to 0 indicates that the bias of the EBK model is low (Krivoruchko et al., 2020). MSE was calculated by dividing the sum of the difference between the measured and the predicted values by the kriging variance (Hwang et al., 2021). In this study, RMSSE between 0.921 and 1.068 is close to 1, and MSE between -0.005 and 0.012 is also close to 0, indicating that the accuracy of the model is acceptable (Table 2).

Table 2. Cross-validation summary statistics from empirical Ordinary kriging (OK)

| Quarter | RMSE (ppm) | ASE (ppm) | RMSSE | MSE |
|---|---|---|---|---|
| Summer in 2020 | 4.200 | 3.900 | 1.068 | -0.005 |
| Autumn in 2020 | 3.519 | 3.339 | 1.048 | 0.012 |
| Winter in 2020-2021 | 3.257 | 3.333 | 0.965 | 0.001 |
| Spring in 2021 | 4.503 | 4.889 | 0.921 | 0.003 |

It is found that the distribution of $XCO_2$ in China is mainly concentrated in the southeast, and the distribution is high in the southeast and low in the northwest. In the northwest, the $XCO_2$ of Xinjiang Uygur Autonomous Region (the most northwestern province in China) is relatively high, mainly showing that except for the low emission of Tarim Basin in winter, the $XCO_2$ emission is high in spring, summer and autumn, compared with other places in Xinjiang province. At the lower left of China is the Tibet Autonomous Region. In 2020, there was a place higher than other places in the west of the region. This place is kangrinboqe, which is a mountain range with rich mineral resources. Northeast China emits more $XCO_2$ in autumn and winter, Southeast China emits more in summer and autumn, and southeast coastal provinces emit more in spring.

## 4. DISCUSSION

In the visualized map, the $XCO_2$ distribution in 2020 and 2021 roughly conforms to the Heihe - Tengchong line. Living space is concentrated in the main cities and urban agglomerations in China, and the ecological space is distributed in the northwest of the Heihe – Tengchong Line (Liu et al., 2017). The northeast region emits the most $XCO_2$ in autumn and winter, which may be due to the large demand for heating. Combined with the visual map of the four seasons, the provincial capital cities have more $XCO_2$. For example, Xi'an, the capital of Shaanxi Province in Central China, has higher $XCO_2$ emissions than other regions all year round. This may be due to industrial pollution in other nearby cities. With the flow of air and wind, a large amount of $XCO_2$ flows into Xi'an. The time range of this study is short, and subsequent studies can be compared and analyzed in combination with the data of GOSAT-2 in the next few years to better show the changing trend of $XCO_2$ or $XCH_4$. Such research will contribute to the formulation of policies to achieve peak carbon dioxide emissions and carbon neutrality.

## 5. CONCLUSIONS

GOSAT-2 data provide $XCO_2$ (unit: ppm) in the atmosphere of China from June 2020 to May 2021. It is of tremendous use in assessing the spatial and temporal aspects of the sources and sinks of man-made and natural carbon dioxide emissions. The conclusion of this study is column-averaged $CO_2$ ($XCO_2$) in the study area remained above 389.61 ppm, and $XCO_2$ was at a high level. The $XCO_2$ is increasing year by year in China. From 2020 to 2021, the mean $XCO_2$ reached the peak in April 2021. The overall level of $XCO_2$ in 2021 is higher than that in 2020. The average value of $XCO_2$ increased from 413.86 ppm in 2020 to 419.59 ppm in 2021, an increase of 5.73 ppm. Its distribution is mainly high in the southeast and low in the northwest.

## REFERENCES

Kuze, A., et al., 2009. Thermal and near infrared sensor for carbon observation Fourier-transform spectrometer on the Greenhouse Gases Observing Satellite for greenhouse gases monitoring. Applied Optics. 48(35), pp. 6716-6733.

Suto, H., et al., 2021. Thermal and near-infrared sensor for carbon observation Fourier transform spectrometer-2 (TANSO-FTS-2) on the Greenhouse gases Observing SATellite-2 (GOSAT-2) during its first year in orbit. Atmospheric Measurement Techniques, 14(3), pp. 2013-2039.

Janardanan, R., et al., 2020. Country-Scale Analysis of Methane Emissions with a High-Resolution Inverse Model Using GOSAT and Surface Observations. Remote Sensing. 12, 375.

Deng, F., et al., 2014. Inferring regional sources and sinks of atmospheric $CO_2$ from GOSAT $XCO_2$ data. Atmospheric Chemistry and Physics. 14, pp. 3703-3727.
Hwang, Y., et al., 2016. Comparative evaluation of $XCO_2$ concentration among climate types within India region using OCO-2 signatures. Spat. Inf. Res. 24, pp. 679-688.
Noël, S., et al., 2021. $XCO_2$ retrieval for GOSAT and GOSAT-2 based on the FOCAL algorithm. Atmospheric Measurement Techniques. 14, pp. 3837-3869.
Gong, G., et al., 2014. Comparison of the accuracy of kriging and IDW interpolations in estimating groundwater arsenic concentrations in Texas. Environmental Research. 130, pp. 59-69.
Krivoruchko, K., et al., 2020. Empirical Bayesian Kriging Implemented in ArcGIS Geostatistical Analyst. December 20, 2020, from https://www.esri.com/NEWS/ARCUSER/1012/files/ebk.pdf.
Hwang, Y., et al., 2021. Comparative Evaluation of Top-Down GOSAT $XCO_2$ vs. Bottom-Up National Reports in the European Countries. Sustainability. 13(12), 6700.
Liu. J., et al., 2017. Classification evaluation and spatial-temporal analysis of "production-living-ecological" spaces in China. Acta Geographica Sinica., 72, pp. 1290-1304.